Input Energy Spectra for Pulse-Like Ground Motions

C. Frau(✉), S. Panella, and M. Tornello

Universidad Tecnológica Nacional, Regional Mendoza, Argentina
cdfrau@frm.utn.edu.ar

Abstract. In energy based seismic design (EBSD) approach, effect of ground motions on structures is considered as an energy input to structures (EI). The usage of energy spectra is an effective tool in energy based seismic design (EBSD) methods, such as the use of design acceleration spectra in force-based and displacement-based methods. The obtention of input energy spectra offers an important advantage to determine the energy input to structures with the effect of ground motions. On the other side, near-fault seismic ground motions are frequently characterized by intense velocity and displacement pulses of relatively long periods that clearly distinguish them from typical far-field ground motions. Intense velocity pulse motions can affect adversely the seismic performance of structures. Based on these ideas, a correlation between the impulsivity level and input energy spectrum is presented in this study, and a new parameter is established for evaluating the input energy power. This correlation may aid to select ground motion for structural analysis in near-fault regions.

Keywords: input energy spectra · pulse-like ground motions · near-fault zones

1 Introduction

Energy concept in seismic design of structures has been widely studied over a half-century period and energy-based methods have always been considered more rational and reliable for the design and assessment of structures under seismic effects when compared to conventional force-based and displacement-based methods (Uang and Bertero 1990; Akbas and Shen 2003). In the energy-based methods earthquake effect is considered as an energy input to structures and this energy input expresses the total energy demand of the earthquake. Making a structure safe is considered as a balance of energy dissipation capacity and earthquake energy demand in these approaches. However, an important question of the energy-based seismic design is to determine the energy input to structures with earthquake motion. Energy-based earthquake resistant design was first proposed by Housner (1956), who studied the seismic energy input to structures using the velocity spectra of elastic systems. Energy-based design parameters were first defined in his research, and these formed a basis for earthquake resistant energy-based design. Some other researchers also made many previous estimations about the input energy concept, and they considered the input energy as an effective tool in earthquake-resistant design

H. Varum et al. (Eds.): IWEBSE 2023, LNCE 236, pp. 216–233, 2023.
https://doi.org/10.1007/978-3-031-36562-1_17

(Uang and Bertero 1990; Fajfar and Fischinger 1990; Manfredi 2001). Zahrah and Hall (1984), Akiyama (1985), Kuwamura and Galambos (1989), Fajfar et al. (1989) made pioneer studies like Housner about seismic energy concepts and they proposed useful analytical and empirical equations for the seismic input energy.

On the other side, it is known that near fault regions are exposed to directivity effects. When a fault ruptures toward a site, a rupture velocity slightly slower than the shear wave velocity produces an accumulation of seismic energy released during rupture (Somerville et al. 1997; Spudich and Chiou 2008); this generally results in a large pulse in the velocity-time series. Thus, near-fault seismic ground motions are frequently characterized by intense velocity and displacement pulses of relatively long periods that clearly distinguish them from typical far-field ground motions. Báez and Miranda (2000) found that the maximum ground velocity and the maximum incremental velocity are the parameters that most influence the structural response.

Intense velocity pulse motions can affect adversely the seismic performance of structures (Bertero et al. 1978; Chopra and Chintanapakdee 2001). Anderson and Bertero (1987) demonstrated that the presence of long acceleration pulses demands higher resistance of structures to stand upright. Malhotra (1999) affirms that the presence of characteristic pulses of acceleration, velocity and displacement can generate greater shear at the base of buildings and greater lateral displacements compared to records that do not have these pulses; the demand for ductility can be much higher and the additional damping added to a structure can be less effective. In structures placed into near-fault zones the damage is caused by a few cycles inelastic strain, they are in coincidence with the long velocity pulses and great amplitude (Alavi and Krawlinker 2001). In opposite, in sites placed far away faults damage is distributed during all time of the record in many cycles with minor inelastic strain (Báez and Miranda 2000).

In energy based seismic design (EBSD) approach, effect of ground motions on structures is considered as an energy input to structures. The earthquake input energy spectra are created combining the maximum input energies of single degree of freedom (SDOF) systems having a certain damping ratio for different natural vibration periods. The determination of input energy spectra is of great importance for the energy based seismic design since the total energy input to structural systems can be practically obtained via these graphs.

The usage of energy spectra is an effective tool in EBSD methods, such as the use of design acceleration spectra in force based and displacement based methods. The obtention of input energy spectra offers an important advantage to determine the energy input to structures with the effect of ground motions.

In EBSD of structures, the energy demand of an earthquake should be less than or, in limit, should be equal to, the energy dissipation capacities possessed by the structure. It is of utmost importance for structural and earthquake engineers that the seismic input energy transmitted to structures is computed exactly.

These concepts suggest assessment the relationship between input energy and impulsivity in ground motions like-pulse. With this target, in this work input energy for impulsive records set are analyzed. The set is taken from the Panella et al. (2017) and it is organized in different impulsivity levels. To evaluate the energy input a new parameter is proposed, it consider the time of the earthquake in delivering the energy. To the end a

matrix to link both parameters (input energy and impulsivity) is presented. The matrix may help to a better selection of record to structural analysis.

2 Ranking of Pulse-Like Ground Motions

2.1 Pulse-Like Ground Motions Classification

Panella et al. (2017) developed a method to identifying and classifying like-pulse ground motions. Departing from a velocity time history of ground motion the "developed length of velocity" *Ldv* is defined as the length reached by the trace of velocity records as if it were "extended" like a string (Eq. 1).

$$Ld_v = \sum_{i=1}^{n} \left(\sqrt{(\Delta t)^2 + (\Delta v_i)^2} \right) \tag{1}$$

where Δt is the time lapse of the record between two successive points $t(i+1) - t(i)$ in *s*, Δvi are velocity increments between $t(i)$ and $t(i+1)$ in *cm/s*, and n is the number of samples in the series. Given the binary character of the target classification (pulse-like or non-pulse) and enough data availability, a binary logistic regression was used to classify the records; *Ldv* and *PGV* (Peak Ground Velocity) were the parameters used (Eq. 2). The logistic regression proved the following predictive equation for the Impulsivity Index by Regression (IPR).

$$\mathrm{IP_R} = \frac{1}{1 + e^{(5 - 0.45\mathrm{PGV} + 0.01\mathrm{Ldv})}} \tag{2}$$

The Impulsivity Index by Regression takes values between 0 and 1. A ground motion qualifies as pulse type if its *IPR* is higher than 0.7 and its *PGV* is higher than 30 cm/s. Below 0.7 the record is non-pulse. It is well-known that several researchers have established as an excluding condition to classify a record as pulse-type that *PGV* should reach a minimum of 30 cm/s [18, 23]. Even though this value is not adequately justified, it imposes a minimum to the power of the pulse for a time velocity series to be classified as pulse-type. The impulsivity level is defined with an indicator based on the development length of velocity and *PGV*; the "Impulsivity Index" *IP* is as follows:

$$\mathrm{IP} = \frac{\mathrm{Ldv}}{\mathrm{PGV}} \tag{3}$$

The definition of *Ldv* captures in a simple and efficient way the impulsive aspect visually detected in a velocity time series. A relatively low *Ldv* value represents an impulsive character, whereas a high *Ldv* value represents a non-pulse or vibratory character. Pulse amplitude also plays an important role: high *PGV* reveal the presence of at least one pulse, whereas low *PGV* "dilute" pulses. In this way, a combination of low *Ldv* values and high *PGV* leads to small *IP* suggesting high impulsivity, while the opposite is the manifestation of a non-pulse character. Once a record is identified as pulse-type by *IPr*, ranks can be established using the value taken by *IP* to classify ground motions into three impulsivity levels: high, medium or moderate, and low (see Table 1); $IP = 35$ divides between pulse and non-pulse.

Table 1. Classification proposed for different impulsivity levels.

Impulsivity Index IP	Impulsivity Level
IP $\leq$ 12	High (H)
12 $<$ IP $\leq$ 20	Medium or Moderate (M)
20 $<$ IP $\leq$ 35	Low (L)

2.2 Database and Ranking of Pulse-Like Ground Motions

For this study we selected a set of 114 impulsive records from Panella et al. database; with IP between 6.5 and 35. The seismic records used correspond to earthquakes in different parts of the world with a moment magnitude between 5.5 and 7.9. Strong motions have a Joyner-Boore distance less than 30 km. In the Appendix 1, Table A-1 shows data for the selected set. Figure 1 shows *IP* in increasing order for the 104 selected records. A continuous variation is seen (between 5 and 35), without jumps; this shows the consistency of the data for subsequent analysis.

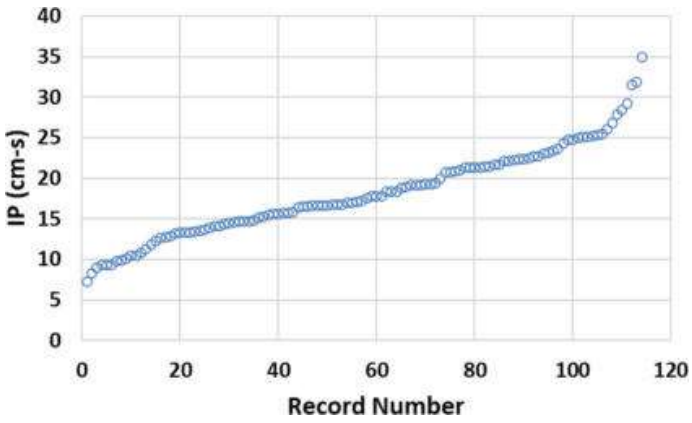

Fig. 1. *IP* in increasing order for the selected records.

3 Energy Spectra

3.1 Elastic Input Energy Spectrum

Starting from the fundamental definition of work, (i.e., the integral of force with respect to displacement) the so-called energy balance equation can be easily obtained by integrating the governing differential equation of motion of a SDOF system subjected to a horizontal ground motion over the relative displacement of the mass with respect to the ground:

$$\int_0^u m\ddot{u}(t)du + \int_0^u c\dot{u}(t)du + \int_0^u ku(t)du = -\int_0^u m\ddot{u}_g(t)du \tag{4}$$

The integral quantities on the left-hand side of this equation identify the different energy components of the structure named as the kinetic energy, the damping energy and

the recoverable strain energy, respectively. The right-hand side of the Equation which is closely associated with the main concern of the present study, expresses the total input energy $EI(t)$.

According to the rules of mathematical analysis, the incremental displacement du can be expressed as which enables integration of the governing equation of motion with respect to duration of earthquake. Accordingly, for a specific earthquake ground motion, the relative energy input to a SDOF system, as well as the other energy components, and be theoretically obtained by integrating the equation of motion over the time (Eq. 5); Fig. 2-a shows the input energy as a time function.

$$\frac{E_I}{m} = \int_0^t \ddot{u_g}(t)\dot{u}(t)dt \tag{5}$$

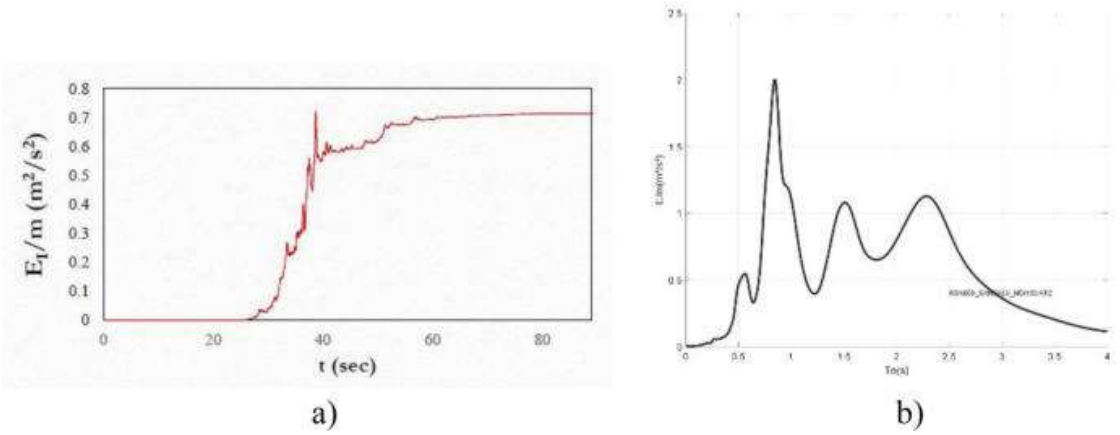

Fig. 2. a) Input energy as a time function for a record with period and damping given; b) Input energy spectrum.

When this process is repeated for various SDOF systems with different periods *Tn* but the same damping ratios, a set of *EI* versus *Tn* elastic input energy spectrum are obtained. In brief definition, the seismic input energy spectra are the graphs which combine the maximum energy input values corresponds to different natural vibration periods of SDOF systems (Fig. 2-b). Figure 3 shows the input energy spectra for some records from the set selected; great variability can be seen.

3.2 Input Energy Power and Input Energy Power Spectrum

Considering input energy for a period given *Ti*, Input Energy Power (*IEP*) is defined as the total input energy divided by the time energy takes to enter (Eq. 6). Because the energy delivery is small at the beginning and end of the records (see Fig. 2-a), to define *IEP* the effective duration is considered. For this Arias Intensity is used; effective duration is time interval between 5% (t_i) and 95%(t_f) (Arias 1970).

$$IEP = \frac{E_I/m}{(t_f - t_i)} = \frac{1}{t_f - t_i}\int_{ti}^{tf} \ddot{u_g}(t)\dot{u}(t)dt \tag{6}$$

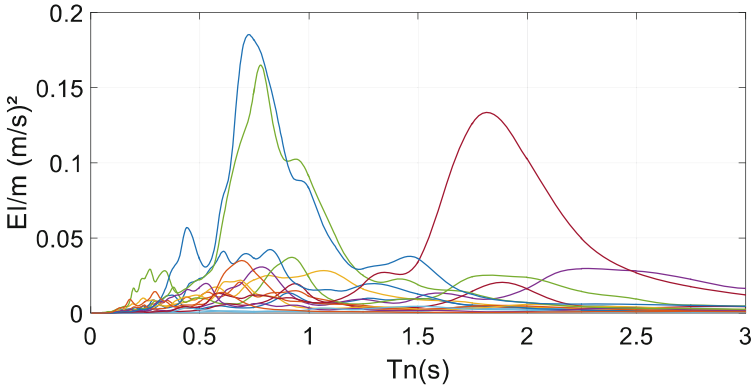

Fig. 3. Input energy spectra for some records from the selected set.

After calculating the *IEP* for each structural period (*Tn*), it is possible to construct the Input Energy Power Spectrum $S_{IEP}(Tn, \zeta)$. This spectrum takes into account, in addition to the energy that enters, the power with which it does so. It must be recognized that the total amount of energy that enters is important, but also the time in which that energy must be dissipated, that is, the power. Figure 4 shows two cases studied where one reaches higher energy but the other reaches higher power. Figure 4 shows two cases studied where once reach higher energy but the other reach higher power.

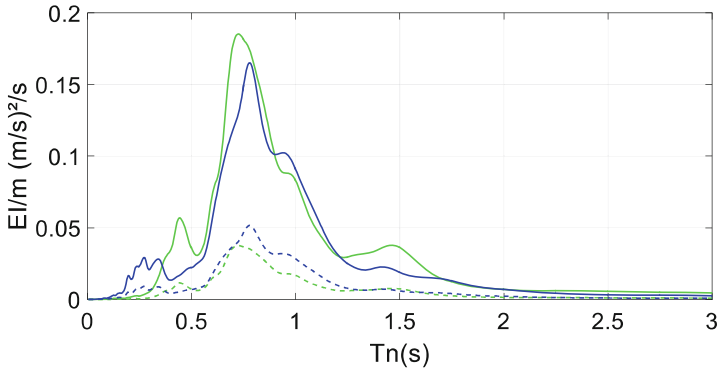

Fig. 4. Input Energy Spectra (continuous line) and Input Energy Power Spectrum $S_{IEP}(Tn, \zeta)$ (dashed line) for two records: RSN569_SANSALV_NGI270 and RSN451_ MORGAN_ CYC285 (See Appendix 1).

4 Energy Spectral Intensity

4.1 Housner Intensity

Housner (1952) defined a spectral intensity from the pseudo-velocity elastic response spectrum, which is obtained from an acceleration record. The Housner Spectral Intensity is defined as (Eq. 7):

$$SI(Housner) = \int_{0.1}^{2.5} Sv(T, \xi)dT \tag{7}$$

where *Sv* is the pseudo-velocity elastic response spectrum, *T* are the structural periods, ζ is the fraction of critical damping and 0.1–2.5 s are the periods that the integral covers. The Housner Spectral Intensity express the relative severity of earthquakes.

4.2 Energy Spectral Intensity

Whit the same idea of Housner Intensity, in this work a new parameter to evaluate the input energy is proposed: the Energy Spectral Intensity (*ESI*). This is defined from the Input Energy Power Spectrum according to following equation (Eq. 8).

$$ESI = \int_{0.1}^{2.5} S_{IEP}(T, \xi) dT \tag{8}$$

ESI quantifies the severity of seismic records by concentrating in a value the input energy and the power with which it does so in an interest periods range. Besides, it allows to compare different records each other; in special when, in many cases, the input energy spectra present great variation from a period to other (see Fig. 2-b). Figure 5 shows an example of how the parameters described above are obtained.

La Fig. 5 muestra un ejemplo de cómo se obtienen los parámetros descritos anteriormente.

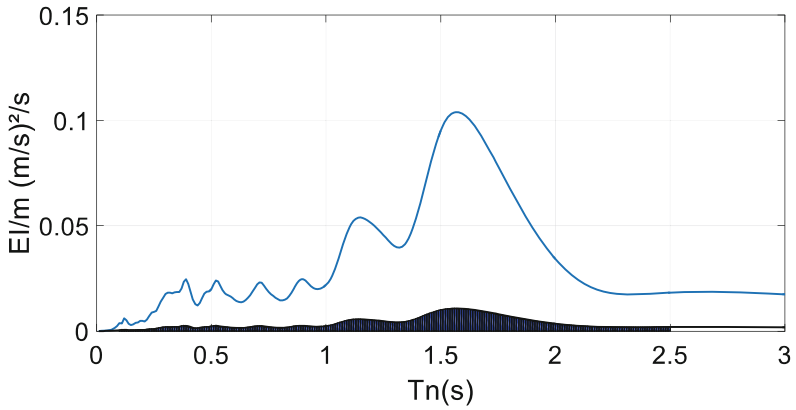

Fig. 5. Example of how the ESI is obtained.

For the set of selected records, the spectral intensity of energy was calculated. Figure 6 shows the values reached by *ESI* in an orderly and increasing manner. A more or less continuous variation without jumps is observed. This means that the selected record set is consistent and covers a wide range of cases.

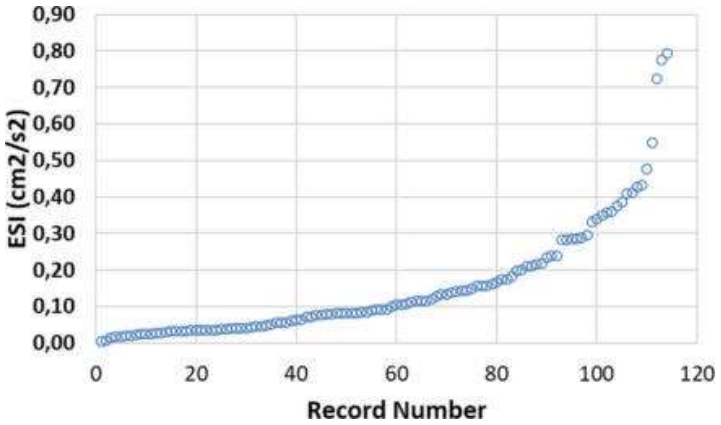

Fig. 6. *ESI* in increasing order for the selected records.

5 Energy and Impulsivity

5.1 Relation Between Energy and Impulsivity

This section investigates the relationship between impulsivity and energy input. For this, the impulsivity index of Panella et al. (2017) and the Energy Spectral Intensity defined in this work were considered. Figure 7 shows a scatter graph where the Impulsivity Index *IP* is represented on the abscissa, while the Energy Spectral Intensity *ESI* is represented on the ordinate.

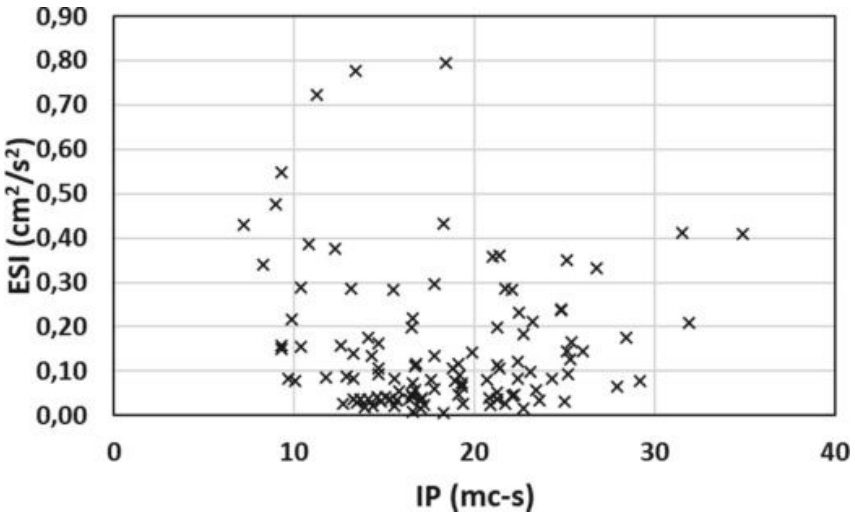

Fig. 7. a) *IP* vs. *ESI* for the selected records.

Figure 7 does not show a direct relationship between the impulsivity of the recording and the spectral intensity of energy. However, it can be stated that the highest energy spectral intensities correspond to records of moderate to high impulsivity ($IP < 20$); thus, records with low impulsivity do not present high *ESI*. Records with low *ESI* present impulsivity of all levels (high, moderate and low). Based on the results obtained, a classification of records according to the power of the energy input (*ESI*) is proposed; It is divided into three levels: High, Moderate and Low according to the limits shown in Table 2.

Table 2. Classification proposed for different Energy Spectral Intensity.

Energy Spectral Intensity (cm^2/s^2)	Input Energy Level
ESI $>$ 0.4	High (H)
0.20 $<$ ESI $\leq$ 0.40	Moderate (M)
ESI $\leq$ 0.20	Low (L)

From the classification of impulsivity and energy input, a matrix is formed to select seismic records for structural analysis that involves impulsivity and the spectral intensity of energy (*ESI*). The matrix combines both parameters and is shown in Table 3.

Table 3. Matrix for selecting records considering impulsivity and energy input.

SELECTION MATRIX		IMPUSIVITY INDEX (cm,s)		
		ID ≤ 12 km	12 < ID ≤ 20	ID >35
ENERGY SPECTRAL INTENSITY (cm^2/s^2)	ESI > 0,40	H_0	H_1	M_1
	0,20 < ESI ≤ 0,40	H_1	M_0	L_1
	ESI ≤ 0,20	M_1	L_1	L_0

With this classification we organized a matrix to select proper impulsive records considering energy input. This matrix combines the key parameters studied: the level impulsivity and Energy Spectral Intensity. This matrix together with the ranking of strong motions pulse-like (see Appendix 1) will allow designers to make more realistic analysis for structures that take place in near-fault regions when Energy-Based Seismic Design is used.

Both magnitudes are represented by 3 levels: (see Table 1 and 2). When Tables 2 and 3 are combined, different kind of interactions appear: a) High demand for energy and impulsivity (H); b) Moderate demand for energy and impulsivity (M); and c) Low demand for energy and impulsivity (L). The subscript zero (0) indicates strong interactions and the subscript one (1) indicates weak interactions. Thus, matrix allows to choose different levels of impulsivity and input energy for structural analysis.

6 Conclusions

A set of impulsive records taken from previous studies on impulsivity was selected that classifies the records according to different levels of impulsivity.

Based on the Elastic Input Energy Spectra, a new parameter was defined to evaluate the energy input of a seismic record that takes into account the power with which the energy enters: the Energy Spectral Intensity.

With the results obtained for the Energy Spectral Intensity, a ranking was proposed according to the levels of the input energy power.

Combining the classification in levels of impulsiveness and spectral energy intensity, a matrix is created to select impulsive registers according to different input energy levels. Records can be chosen from the Appendix 1.

Acknowledgements. The authors wish to express their gratitude to the Regional Center of Technological Development for Construction, Seismology and Earthquake Engineering (CeReDeTeC) of National Technological University (Argentina) for their support for the present study.

Appendix 1

Table A-1. Parameters of the records used in this work.

N°	ID	Nombre de Sismo	Earthquake Magnitude	J-B Dist. (km)	PGA (g)	PGV (cm/s)	IP (cm-s)	IPR	Record Duration (s)	Time IA 5–95% (s)	ESI (cm^2/s^2)
1	174	RSN182 IMPVALL.H H-E07230	6,53	0.6	0,47	113,1	7,2	1,0	36,8	4,8	0,429
2	159	RSN171 IMPVALL.H H-EMO270	6.53	0.1	0.30	92.6	8.3	1,0	40,0	6,7	0,340
3	335	RSN568 SANSALV GIC090	5.80	2,1	0.70	79.9	9.0	1.0	9.0	4,3	0,477
4	158	RSN171 IMPVALL.H H-EMO000	6,53	0,1	0,32	73,0	9,3	1.0	40,0	8.2	0,158
5	172	RSN181 IMPVALL.H H-E06230	6,53	0,0	0,45	113,6	9,3	1,0	39,1	8,7	0,148
6	336	RSN568 SANSALV GIC180	5,80	2.1	0.42	62,4	9.3	1,0	9,0	3,1	0,549
7	168	RSN179 IMPVALL.H H-E04230	6.53	4.9	0.37	80.4	9.7	1,0	39,1	10,3	0,082
8	104	RSN150 COYOTELK G06230	5,74	0,4	0.42	44,4	9.9	1.0	27,1	3,2	0,216
9	157	RSN170 IMPVALL.H H-ECC092	6,53	7.3	0.24	73,4	10,1	1,0	40,0	13.2	0,079
10	170	RSN180 IMPVALL.H H-E05230	6,53	1,8	0.38	96.9	10,4	1,0	39.3	9.5	0,156
11	337	RSN569 SANSALV NGI180	5.80	3,7	0,40	56,4	10,4	1.0	20,3	6.2	0.289
12	338	RSN569 SANSALV NGI270	5.80	3,7	0,53	73,0	10.8	1,0	20,3	4.9	0,387

(*continued*)

Table A-1. (*continued*)

N°	ID	Nombre de Sismo	Earthquake Magnitude	J-B Dist. (km)	PGA (g)	PGV (cm/s)	IP (cm-s)	IPR	Record Dura-tion (s)	Time IA 5–95% (s)	ESI (cm^2/s^2)
13	382	RSN723 SUPER.B B-PTS225	6,54	1,0	0,43	134,4	11,3	1.0	22,3	10,6	0,723
14	273	RSN412 COALINGA D-PVY045	5,77	13.2	0.58	37.5	11.8	1,0	21,7	3.8	0,085
15	329	RSN529 PALMSPR NPS210	6.06	0.0	0.69	66.0	12.3	1,0	20.2	4.8	0,375
16	173	RSN182 IMPVALL.H H-E07140	6.53	0.6	0,34	51,7	12,6	1,0	36.8	6.8	0,157
17	385	RSN730 SPITAK GUK000	6.77	24,0	0,20	28,4	12,7	1,0	20,0	10,5	0,026
18	72	RSN147 COYOTELK G02140	5.74	8,5	0.26	32,0	12.9	1.0	26,8	4,0	0.089
19	328	RSN527 PALMSPR MVH135	6,06	3,6	0,22	40,0	13,2	1.0	20,1	6,7	0,285
20	177	RSN184 IMPVALL.H H-EDA270	6,53	5,1	0,35	75,6	13,3	1,0	39.1	7,0	0,138
21	324	RSN502 MTLEWIS HVR090	5.60	12,4	0 .15	19.0	13.3	0.7	40,0	5,1	0,036
22	334	RSN564 GREECE H-KAL-NS	6,20	6,5	0.24	33.5	13.3	1,0	29,2	5,0	0,083
23	294	RSN451 MORGAN CYC285	6,19	0,2	1,30	78.5	13,4	1.0	30,0	3,2	0,776
24	154	RSN161 IMPVALL.H H-BRA315	6,53	8,5	0,22	40.9	13,5	1,0	37,8	14,4	0,028
25	160	RSN173 IMPVALL.H H-E10050	6.53	8.6	0.17	50,7	13.7	1,0	37,0	12,8	0,036
26	153	RSN161 IMPVALL.H H-BRA225	6,53	8,5	0.16	36.6	13.9	1.0	37,8	14.9	0,019
27	77	RSN148 COYOTELK G03140	5,74	6,8	0,26	29.6	14,1	1,0	26.8	8,7	0,035

(*continued*)

Table A-1. (*continued*)

N^o	ID	Nombre de Sismo	Earthquake Magnitude	J-B Dist. (km)	PGA (g)	PGV (cm/s)	IP (cm-s)	IPR	Record Duration (s)	Time IA 5–95% (s)	ESI (cm^2/s^2)
28	279	RSN415 COALINGA D-TSM360	5,77	3,7	1,02	47,8	14.1	1,0	21,7	3,7	0,176
29	345	RSN614 WHITTIER.A A-BIR180	5,99	14,9	0,35	39.9	14.3	1.0	28,6	3,8	0,134
30	265	RSN411 COALINGA D-PVP360	5,77	13,2	0.41	20,2	14,4	0.8	20,6	4.5	0,021
31	213	RSN316 WESMORL PTS225	5,90	16,5	0,23	55,6	14,6	1,0	41,7	15,2	0,042
32	171	RSN181 IMPVALL.H H-E06140	6,53	0.0	0,45	67,0	14,7	1,0	39,1	11,5	0,162
33	212	RSN292 ITALY A-STU270	6,90	6.8	0.32	72,0	14,7	1.0	39.3	15.2	0,093
34	391	RSN764 LOMAP GOF160	6,93	10,3	0.29	43.4	14.7	1,0	40,0	8.9	0.107
35	381	RSN722 SUPER.B B-KRN360	6,54	18,5	0.14	29.6	14.8	1,0	22,0	12,4	0,032
36	179	RSN185 IMPVALL.H H-HVP225	6,53	5,4	0.26	53.2	15.1	1.0	37,8	11,8	0,041
37	180	RSN185 IMPVALL.H H-HVP315	6.53	5,4	0.22	51.5	15.3	1,0	37,8	12.8	0,036
38	278	RSN415 COALINGA D-TSM270	5,77	3,7	0.78	47.5	15.5	1.0	21,7	4.0	0,283
39	161	RSN173 IMPVALL.H H-E10320	6,53	8,6	0.23	46.4	15,6	1.0	37,0	12.0	0,082
40	349	RSN668 WHITTIER.A A-NOR36	5.99	14,4	0.25	26.3	15,6	0.9	30,2	9.4	0,021
41	187	RSN214 LIVERMOR A-KOD180	5,80	15.2	0,15	20,8	15,7	0.8	20,9	10.4	0,035
42	346	RSN615 WHITTIER A A-DWN18	5,99	15,0	0,21	30,7	15,7	1,0	40,0	9.2	0,033

(*continued*)

Table A-1. (*continued*)

N°	ID	Nombre de Sismo	Earthquake Magnitude	J-B Dist. (km)	PGA (g)	PGV (cm/s)	IP (cm-s)	IPR	Record Dura-tion (s)	Time IA 5–95% (s)	ESI (cm^2/s^2)
43	347	RSN645 WHITTIER.A A-OR2010	5,99	19.8	0,23	31,5	15.8	1,0	32,1	8.0	0.055
44	217	RSN33 PARKF TMB205	6,19	16,0	0,36	22,3	16,4	0.8	30,4	4,4	0.037
45	175	RSN183 IMPVALL.H H-E08140	6,53	3.9	0,61	54,5	16,5	1,0	37,6	6.8	0,199
46	210	RSN285 ITALY A-BAG270	6,90	8,1	0,19	34,7	16,5	1,0	36,8	16,1	0,046
47	105	RSN150 COYOTELK G06320	5,74	0,4	0,32	25,4	16,6	0,9	27,1	3.5	0,073
48	182	RSN192 IMPVALL H H-WSM180	6,53	14,8	0,11	22,6	16,6	0,8	40,0	25.6	0,007
49	327	RSN527 PALMSPR MVH045	6,06	3,6	0,22	31,0	16,6	1,0	20,1	5.1	0.220
50	348	RSN652 WHITTIER.A A-DEL000	5.99	22,4	0,30	32,4	16,6	1,0	29,7	11.2	0,041
51	176	RSN183 IMPVALL. H H-E08230	6,53	3,9	0,47	52,1	16,7	1,0	37,6	5.8	0,112
52	323	RSN496 NAHANNI S2330	6,76	0,0	0,36	32,0	16,7	1,0	10,0	7.3	0,056
53	295	RSN459 MORGAN G06090	6,19	9,9	0,29	36,5	16.8	1,0	30,0	6.5	0,117
54	165	RSN178 IMPVALL H H-E03230	6.53	10,8	0,22	43,3	17,0	1.0	39,6	14.1	0,016
55	322	RSN496 NAHANNI S2240	6,76	0,0	0,52	29.6	17,0	1,0	10,0	7.2	0,034
56	91	RSN149 COYOTELK G04360	5,74	4,8	0,25	31.9	17,1	1,0	27,1	11,0	0,040
57	188	RSN235 MAMMOTH J J-MLS25-	5,69	1,5	0,39	24,2	17,2	0.9	30,0	3.9	0,023
58	147	RSN159 IMPVALL.H H-AGR273	6,53	0,0	0,19	41.8	17,6	1.0	28,4	12,4	0,081

(*continued*)

Table A-1. (*continued*)

N°	ID	Nombre de Sismo	Earthquake Magnitude	J-B Dist. (km)	PGA (g)	PGV (cm/s)	IP (cm-s)	IPR	Record Duration (s)	Time IA 5–95% (s)	ESI (cm^2/s^2)
59	145	RSN158 IMPVALL.H H-AEP045	6,53	0,0	0,31	42.8	17.8	1.0	14,7	9.8	0,133
60	293	RSN451 MORGAN CYC195	6.19	0,2	0,71	52,9	17,8	1,0	30,0	4,1	0.295
61	296	RSN461 MORGAN HVR240	6.19	3,5	0,31	39,4	17,8	1,0	40,0	10,7	0,061
62	181	RSN192 IMPVALL. H H-WSM090	6,53	14,8	0,08	22,2	18,3	0,7	40,0	24,7	0,005
63	342	RSN585 BAJA CPE251	5.50	3,4	0,91	55,4	18,3	1,0	40,0	4,2	0,431
64	400	RSN77 SFERN PUL164	6,61	0,0	1,22	114,5	18,4	1,0	41,7	7,0	0,794
65	156	RSN170 IMPVALL.H H-ECC002	6,53	7,3	0,21	38,4	18,8	1,0	40,0	10,4	0,106
66	164	RSN178 IMPVALL. H H-E03140	6,53	10,8	0,27	48,0	18,9	1,0	39,6	11.9	0,078
67	344	RSN611 WHITTIER.A A-CAS000	5.99	18,3	0,32	29,5	19,1	0,9	31,1	8.0	0,048
68	383	RSN723 SUPER.B B-PTS315	6,54	1,0	0,38	53,2	19,1	1,0	22,3	11.0	0,117
69	330	RSN540 PALMSPR WWT180	6,06	0,0	0,48	38,5	19.2	1,0	20,1	5.5	0,092
70	183	RSN20 NCALIF.FH H-FRN044	6.50	26,7	0,16	36,1	19,3	1,0	40,0	17,3	0,072
71	390	RSN763 LOMAP GIL067	6,93	9,2	0,36	31,1	19,3	1,0	40,0	5.0	0,065
72	207	RSN266 VICT CHI102	6,33	18,5	0,15	26,0	19,4	0,8	26,9	16,4	0,027
73	169	RSN180 IMPVALL.H H-E05140	6,53	1,8	0,53	48,9	19,9	1,0	39,3	8,3	0,141
74	361	RSN692 WHITTIER A A-EJS048	5.99	11,5	0,47	34,4	20,7	1,0	37.8	5.8	0.079

(*continued*)

Table A-1. (*continued*)

N°	ID	Nombre de Sismo	Earthquake Magnitude	J-B Dist. (km)	PGA (g)	PGV (cm/s)	IP (cm-s)	IPR	Record Dura-tion (s)	Time IA 5–95% (s)	ESI (cm^2/s^2)
75	286	RSN448 MORGAN AND250	6.19	3,2	0,42	25,4	20,8	0,8	28,4	6,9	0,038
76	214	RSN316 WESMORL PTS315	5,90	16,5	0,15	32,7	20,9	1,0	41,7	18,7	0,024
77	341	RSN585 BAJA CPE161	5.50	3,4	1,28	46,4	21,0	1,0	40,0	3,2	0 ,358
78	184	RSN20 NCALIF.FH H-FRN314	6.50	26,7	0,20	26,2	21,3	0.8	40,0	19.4	0,036
79	167	RSN179 IMPVALL.H H-E04140	6.53	4,9	0,48	39,7	21.3	1,0	39,1	6.7	0,200
80	196	RSN250 MAMMOTH.L L-LUL09	5.94	9,7	0,41	34,1	21,3	1,0	26.0	7.1	0,115
81	223	RSN359 COALINGA.H H-PV109	6,36	24,8	0.23	27,5	21.3	0,8	60.0	10.9	0,051
82	68	RSN126 GAZLI GAZ000	6.80	3,9	0,70	66,3	21,4	1,0	13,5	6,4	0,360
83	287	RSN448 MORGAN AND340	6.19	3,2	0.29	27.8	21,4	0.8	28,4	5.2	0,106
84	69	RSN126 GAZLI GAZ090	6.80	3,9	0,86	67,7	21,7	1,0	13,5	7.0	0,286
85	343	RSN595 WHITTIER A A-JAB297	5,99	10,3	0.22	28.3	21,7	0.8	34,3	10,4	0,025
86	244	RSN407 COALINGA D-OLC270	5,77	2,0	0,84	40,0	22,1	1,0	21,2	2.8	0,283
87	362	RSN692 WHITTIER A A-EJS318	5,99	11,5	0,46	31,6	22.1	0,9	37,8	6.0	0.044
88	90	RSN149 COYOTELK G04270	5.74	4.8	0,23	25,8	22,2	0,7	27,1	8,2	0,047
89	67	RSN125 FRIULLA A-TMZ270	6,50	15,0	0.32	30,5	22,4	0,9	36,4	4,9	0,121

(*continued*)

Table A-1. (*continued*)

N°	ID	Nombre de Sismo	Earthquake Magnitude	J-B Dist. (km)	PGA (g)	PGV (cm/s)	IP (cm-s)	IPR	Record Dura-tion (s)	Time IA 5–95% (s)	ESI (cm^2/s^2)
90	162	RSN174 IMPVALL.H H-E11230	6,53	12,6	0.38	44,6	22,4	1,0	39,4	7,9	0,083
91	387	RSN753 LOMAP CLS000	6,93	0.2	0.65	56,0	22,5	1.0	40,0	6,9	0,233
92	333	RSN558 CHALFANT. A A-ZAK36	6,19	6,4	0.40	44,7	22,7	1,0	40,0	8,1	0,183
93	386	RSN737 LOMAP AGW000	6,93	24,3	0,17	33,5	22,7	0,9	60,0	21,2	0,016
94	320	RSN495 NAHANNI S1010	6,76	2,5	1,11	43.9	23,1	1,0	10,3	7,5	0,099
95	215	RSN319 WESMORL WSM090	5,90	6,2	0,38	44,2	23,2	1,0	65,0	6,9	0,210
96	146	RSN159 IMPVALL.H H-AGR003	6,53	0,0	0.29	35,3	23,4	0.9	28,4	13,3	0,057
97	379	RSN721 SUPER.B B-ICC000	6,54	18.2	0,36	48,1	23,6	1,0	60,0	28,0	0,033
98	195	RSN250 MAMMOTH.L L-LUL00	5,94	9.7	0,95	30,3	24,3	0.8	26,0	6,5	0,082
99	178	RSN184 IMPVALL.H H-EDA360	6,53	5,1	0,48	41,0	24,8	1,0	39,1	6,6	0,238
100	388	RSN753 LOMAP CLS090	6.93	0.2	0,48	47,6	24.8	1.0	40,0	7,9	0,239
101	380	RSN721 SUPER.B B-ICC090	6,54	18.2	0,26	41.8	25,0	1.0	60,0	35,7	0,032
102	71	RSN143 TABAS TAB-T1	7,35	1,8	0.86	123,6	25,1	1,0	32,8	16,3	0,351
103	321	RSN495 NAHANNI S1280	6,76	2.5	1,20	40,6	25,1	1,0	10,3	7,3	0,145
104	389	RSN755 LOMAP CYC285	6,93	20,0	0,49	40,6	25,2	1.0	40,0	12,2	0,092

(*continued*)

Table A-1. (*continued*)

N°	ID	Nombre de Sismo	Earthquake Magnitude	J-B Dist. (km)	PGA (g)	PGV (cm/s)	IP (cm-s)	IPR	Record Dura-tion (s)	Time IA 5–95% (s)	ESI (cm^2/s^2)
105	331	RSN540 PALMSPR WWT270	6,06	0,0	0.63	30,8	25.3	0,7	20,1	3.4	0,127
106	332	RSN558 CHALFANT.A A-ZAK27	6,19	6,4	0,45	36,9	25,4	0.9	40,0	6,2	0,166
107	224	RSN367 COALINGA.H H-PVB04	6,36	7,7	0.30	39,4	26,0	0.9	58,1	8,3	0,144
108	225	RSN368 COALINGA.H H-PVY04	6,36	7,7	0.60	60,5	26,8	1,0	58,1	8,2	0,332
109	211	RSN292 ITALY A-STU000	6.90	6.8	0,23	37,0	27.9	0.8	39.3	15,0	0,064
110	216	RSN319 WESMORL WSM180	5,90	6.2	0,50	35,8	28,4	0,7	65,0	6.1	0,176
111	384	RSN725 SUPER.B B-POE270	6,54	11,2	0,48	41.3	29.2	0.8	22,3	13,7	0,078
112	70	RSN143 TABAS TAB-L1	7,35	1.8	0,85	99,1	31,5	1,0	32.8	16,5	0,412
113	148	RSN160 IMPVALL.H H-BCR140	6,53	0,4	0.60	46.8	31.9	0.8	37,8	9.6	0,210
114	401	RSN77 SFERN PUL254	6,61	0.0	1,24	57.4	34.9	0,7	41.7	7,3	0,410

References

Uang, C.M., Bertero, V.V.: Evaluation of seismic energy in structures. Earthq. Eng. Struct. Dyn. **19**(1), 77–90 (1990)

Akbas, B., Shen, J.: Earthquake-resistant design (EQRD) and energy concepts. Tech. J. Turk. Chamb. Civ. Eng., 2877–2901, Article no. 192 (2003). (in Turkish)

Housner, G.W.: Limit design of structures to resist earthquakes. In: Proceedings of the First World Conference on Earthquake Engineering, Oakland, California, USA, pp. 186–198 (1956)

Fajfar, P., Fischinger, M.A.: Seismic procedure including energy concept. In: Ninth European Conference on Earthquake Engineering (ECEE), Moscow, vol. 2, pp. 312–321 (1990)

Manfredi, G.: Evaluation of seismic energy demand. Earthq. Eng. Struct. Dyn. **30**(4), 485–499 (2001)

Zahrah, T.F., Hall, W.J.: Earthquake energy absorption in SDOF structures. J. Struct. Eng. **110**(8), 1757–1772 (1984)

Akiyama, H.: Earthquake-Resistant Limit-State Design for Buildings. University of Tokyo Press, Japan (1985)

Kuwamura, H., Galambos, T.V.: Earthquake load for structural reliability. J. Struct. Eng. **115**(6), 1446–1462 (1989)

Fajfar, P., Vidic, T., Fischinger, M.: Seismic demand in medium- and long-period structures. Earthq. Eng. Struct. Dyn. **18**(8), 1133–1144 (1989)

Somerville, P.G., Smith, N.F., Graves, R.W., Abrahamson, N.A.: Modification of empirical strong ground motion attenuation relations to include the amplitude and duration effects of rupture directivity. Seismol. Res. Lett. **68**,199–222 (1997)

Spudich, P., Chiou, B.S.J.: Directivity in NGA earthquake ground motions: analysis using isochrone theory. Earthq. Spectra **24**(1), 279–98 (2008)

Baez, J.I., Miranda, E.: Amplification factors to estimate inelastic displacement demands for the design of structures in the near field. In: 12th World Conference in Earthquake Engineering, New Zealand, Paper 1561 (2000)

Bertero, V.V., Mahin, S.A., Herrera, R.A.: Aseismic design implications of San Fernando earthquake records. Earthq. Eng. Struct. Dyn. **6**(1), 31–42 (1978)

Chopra, A.K., Chintanapakdee, C.: Comparing response of SDF systems to near- fault and far-fault earthquake motions in the context of spectral regions. Earthq. Eng. Struct. Dyn. **30**, 1769–1789 (2001)

Anderson, J.C., Bertero, V.V.: Uncertainties in establishing design earthquakes. J. Struct. Eng. **113**(8), 1709–1724 (1987)

Malhotra, P.K.: Response of building to near-field pulse-like ground motions. Earthq. Eng. Struct. Dyn. **28**, 1309–1326 (1999)

Alavi, B., Krawinkler, H.: Effects of near-fault ground motions on frame structures. Technical report Blume Center Report 138, Stanford, California (2001)

Panella, D.S., Tornello, M.E., Frau, C.D.: A simple and intuitive procedure to identify pulse-like ground motions. Soil Dyn. Earthq. Eng. **94,** 234–243 (2017)

Arias, A.: A measure of earthquake intensity. In: Hansen, R. (ed.) Seismic Design for Nuclear Power Plants, pp. 438–483. MIT Press, Cambridge (1970)

Housner, G.W.: Intensity of ground motion during strong earthquakes. Earthquake Research Laboratory. California Institute of Technology (1952)